Table 1. Univariate Analysis of Recipient Risk Factors for 3-Month Patient Survival

Risk Factor	n	3-Month Survival (%)	P Value
Recipient age			
<50 y	54	85.2	.3142
≥ 50 y	31	93.5	
Recipient sex			
Male	45	86.7	.7431
Female	40	90.0	
MELD score			
< 25	59	93.2	.01752
≥ 25	21	71.4	
Diagnosis			
BA	8	75.0	.822
CMD	6	100.0	
FHF	11	90.9	
LC (Other)	12	91.7	
LC (Viral)	24	87.5	
Other	2	100.0	
PBC	7	100.0	
PSC	2	100.0	
Re-LTx	13	76.9	

Abbreviations: MELD, Model for End-stage Liver Disease; BA, biliary atresia; CMD, congenital metabolic disorders; FHF, fulminant hepatic failure; LC, liver cirrhosis; PBC, primary biliary cirrhosis; PSC, primary sclerosing cholangitis; Re-LTx, retransplantation.

sodium level (≥ 160 mEq/L), total bilirubin (≥ 2.0 mg/dL), aspartate aminotransferase (AST) and alanine aminotransferase (ALT) (≥ 200 IU/I), body mass index (BMI; ≥ 28 kg/m^2), macrosteatosis (≥ 20%), cold ischemia time (CIT; ≥10 hours), warm ischemia time (≥50 minutes), and use of a split liver (Table 2). Subgroup analysis affecting for 3-month survival was performed dividing the recipients based upon the number of significant risk factors (RFs).

Statistical analyses were performed with software "R version 2.13.0"; univariate analysis with the Fisher exact test and multivariate analysis with logistic regression analysis. P values less than .05 were considered statistically significant.

RESULTS

Patient survival was 91.8%, 89.4%, and 88.2%, at 1, 2 and 3 months respectively. Upon univariate analysis significantly worse 3-month survival rates. Center were associated with MELD score ≥ 25 ($P = .018$), donor age ≥ 55 years ($P = .040$), and CIT ≥10 hours ($P = .00013$), (Tables 1 and 2). Upon multivariate analysis, three factors independently worsened 3-month survival rates: MELD score ≥ 25 ($P = .0133$, OR = 12.3, 95% confidence interval (CI) 1.7–90.3), donor age ≥ 55 years ($P = .013$, OR = 14.0, 95% CI = 1.6–119.5), and CIT ≥ 10 hours ($P = .0024$, OR = 67.6, 95% CI = 4.5–1024.9 (Table 3).

Table 2. Univariate Analysis of Donor Risk Factors for 3-Month Patient Survival

Risk Factor	n	3-Month Survival	P Value	Risk Factor	n	3-Month Survival	P Value
Donor age				Na			
< 55	66	92.4	.04025	< 160	77	88.3	1
≥ 55	19	73.7		≥ 160	8	87.5	
Donor sex				T-Bil			
Male	47	91.5	.3311	< 2.0	71	90.1	.3574
Female	38	84.2		≥ 2.0	14	78.6	
Cause of death				AST			
CVA	47	89.4	.6808	< 200	81	88.9	.3997
MVA	19	78.9		≥ 200	4	75.0	
				ALT			
Other	6	100.0		< 200	82	87.8	1
Suicide	11	90.9		≥ 200	3	100.0	
				BMI			
Tumor	2	100.0		< 25	63	88.9	.7141
CPR				≥ 25	22	86.4	
< 10 min	53	84.9	.3108	Steatosis			
≥ 10 min	31	93.5		< 20%	58	93.1	.1217
BP < 60				≥ 20%	7	71.4	
< 2H	78	89.7	.1899	Graft			
≥ 2H	7	71.4		Whole	78	87.2	.592
ICU stay				Split	7	100.0	
< 7 days	38	92.1	.5007	CIT			
≥ 7 days	47	85.1		< 600 min	57	98.2	.00013
Dopamine				≥ 600 min	28	67.9	
< 15 gamma	57	87.7	1	WIT			
≥ 15 gamma	28	89.3		< 50 min	58	89.7	.6932
Vasopressor				≥ 50 min	21	85.7	
0–1 drug	42	88.1	1				
≥ 2 drug	43	88.4					

Abbreviations: Na, sodium; T-bil, total bilirubin; CVA, cerebrovascular accident; AST, aspartate aminotransferase; MVA, motor vehicle accident; ACT, alanine aminotransferase; BP, blood pressure; ICU, intensive care unit; BMI, body mass index; CPR, cardiopulmonary resucitation, CIT, cold ischemia time; WIT, warm ischemia time.

Table 3. Multivariate Analysis For 3-Month Patient Survival

	Coefficient (SE)	Odds Ratio [95% CI]	P Value
MELD score ≥ 25	4.213 (1.387)	12.3 [1.7–90.3]	.0133
Donor age ≥ 55y	2.514 (1.015)	14.0 [1.6–119.5]	.0159
CIT ≥ 600 min	2.639 (1.094)	67.6 [4.5–1024.9]	.0024

Abbreviations: SE, standard error; CI, confidence interval; MELD, Model for End-stage Liver Disease; CIT, cold ischemia time.

When the recipients were divided into four subgroups based on the number of those three RFs, 3-month survival rates of the recipients with 0, 1, 2, and 3 positive RFs were 100% (n = 34), 94.4% (n = 36), 53.8% (n = 13), and 0% (n = 2), respectively ($P < .0001$). When recipients with a CIT < 10 hours had another 1 or 2 RFs, the 3-month survival rates were 100% and 66.7%, whereas among those with CIT ≥ 10 hours, another 1 and 2 RFs yielded 3-month survival rates of 50% and 0% respectively.

DISCUSSION

A number of studies over the past 2 decades have shown that both prolonged CIT and older age are major deleterious factors worsening early recipient outcomes.[1-5] Several recent studies showed recipient factors, especially MELD score in association with extended donor criteria, also adversely impact recipient outcomes.[6-8] Thus, the importance of analyzing both donor and recipient factors simultaneously has been emphasized to match donors and recipients to compensate for their risks.

From this study, MELD score, CIT, and donor age were observed to independently impact 3-month recipient survival rates. Subgroup analysis showed recipients with more RFs to have inferior 3-month survival; however, it was more than 66.7% when CIT was maintained within 10 hours. To minimize CIT, further efforts to reduce transportation time and to adjust donor and recipient operative times are mandatory. The allocation system must be revised to give priority to the local area in the future when more deceased donors become available.

In conclusion, because it is not realistic to eliminate patients with high MELD scores or older donors when there is a chance for a recipient, minimizing CIT is the first priority to improve recipient outcomes in Japan. In the long-term, we must promote an increased number of deceased donors to reduce the MELD score of the recipients by shortening the waiting time, and revise the allocation system to minimize CIT by giving priority to the local area.

REFERENCES

1. Wall WJ, Mimeault R, Grant DR, et al: The use of older donor livers for hepatic transplantation. Transplantation 49:377, 1990
2. Alexander JW, Vaughn WK: The use of "marginal" for organ transplantation: the influence of donor age on outcome. Transplantation 51:135, 1991
3. Furukawa H, Todo S, Imventarza O, et al: Effect of cold ischemia time on the early outcome of human hepatic allografts preserved with UW solution. Transplantation 51:1000, 1991
4. Porte RJ, Ploeg RJ, Hansen R, et al: Long-term graft survival after liver transplantation in the UW era: late effects of cold ischemia and primary dysfunction. European Multicentre Study Group. Transplant Int 11:S164, 1998
5. Feng S, Goodrich NP, Bragg-Gresham JL, et al: Characteristics associated with liver graft failure: the concept of a donor risk index. Am J Transplant. 6:783, 2006
6. Cameron AM, Ghobrial RM, Yersiz H, et al: Optimal utilization of donor grafts with extended criteria: a single-center experience in over 1000 liver transplants. Ann Surg 243:748, 2006
7. Silberhumer GR, Pokorny H, Hubert H, et al: Combination of extended donor criteria and changes in the model for end-stage liver disease score predict patient survival and primary dysfunction in liver transplantation: a retrospective analysis. Transplantation 83:588, 2007
8. Briceño J, Ciria R, de la Mata M, et al: Prediction of graft dysfunction based on extended criteria donors in the model for end-stage liver disease score era. Transplantation 90:530, 2009

Long-Term Hepatic Allograft Acceptance Based on CD40 Blockade by ASKP1240 in Nonhuman Primates

T. Oura[a], K. Yamashita[a,]*, T. Suzuki[a],
D. Fukumori[a], M. Watanabe[a], G. Hirokata[a],
K. Wakayama[a], M. Taniguchi[a], T. Shimamura[a],
T. Miura[b], K. Okimura[b], K. Maeta[b], H. Haga[c],
K. Kubota[c], A. Shimizu[d], F. Sakai[e], H. Furukawa[a]
and S. Todo[a,]*

[a] Department of General Surgery, Hokkaido University
Graduate School of Medicine, Sapporo, Japan
[b] Pharmacological Research Laboratories, Kyowa Hakko
Kirin Co., Ltd., Shizuoka, Japan
[c] Department of Surgical Pathology, Hokkaido University
Hospital, Sapporo, Japan
[d] Department of Pathology, Nippon Medical School, Tokyo,
Japan
[e] Astellas Phama Inc., Tsukuba, Japan
*Corresponding authors: Satoru Todo, and Kenichiro
Yamashita, stodo@med.hokudai.ac.jp and
kenchan@med.hokudai.ac.jp

Blockade of the CD40–CD154 costimulatory signal is an attractive strategy for immunosuppression and tolerance induction in organ transplantation. Treatment with anti-CD154 monoclonal antibodies (mAbs) results in potent immunosuppression in nonhuman primates (NHPs). Despite plans for future clinical use, further development of these treatments was halted by complications. As an alternative approach, we have been focusing on the inhibition of the counter receptor, CD40 and have shown that a novel human anti-CD40 mAb, ASKP1240, markedly prolongs renal allograft survival in NHPs, although allografts eventually underwent chronic allograft nephropathy. On the basis of our previous findings that a CD40–CD154 costimulation blockade induces tolerance to hepatic, but not cardiac, allografts in rodents, we tested here our hypothesis that a blockade of CD40 by ASKP1240 allows acceptance of hepatic allografts in NHPs. A 2-week ASKP1240 induction treatment prolonged liver allograft survival in NHPs; however, the graft function deteriorated due to chronic rejection. In contrast, a 6-month ASKP1240 maintenance monotherapy efficiently suppressed both cellular and humoral alloimmune responses and prevented rejection on the hepatic allograft. No serious side effects, including thromboembolic complications, were noted in the ASKP1240-treated monkeys. We conclude that CD40 blockade by ASKP1240 would be a desirable immunosuppressant for clinical liver transplantation.

Introduction

Costimulation blockade is an effective strategy for preventing allograft rejection in experimental transplantations (1, 2). Among other examples, the inhibition of CD40–CD154 pathway induced tolerance in rodents (3), and the administration of anti-CD154 monoclonal antibodies (mAbs), such as hu5C8, IDEC-131 or ABI793, markedly prolonged kidney allograft survival in nonhuman primates (NHPs) (4–6). Although clinical applications were anticipated, further research was discontinued because these mAbs stimulated platelet (PLT) activation and caused thromboemboli (7,8). As an alternative, we and other researchers have considered the partner molecule, CD40. The anti-CD40 chimeric mAbs ch5D12 and chi220 were shown to prolong kidney allograft survival in NHPs (9,10). As a single agent, however, they were less effective than anti-CD154 mAbs for prolonging graft survival.

ASKP1240 is a newly developed fully human anti-CD40 mAb, which interrupts the CD40–CD154 axis by masking, does not cause antibody-dependent cell-mediated cytotoxicity or complement-dependent cytotoxicity, and consists of type 4 immunoglobulin G (11). In previous studies, we showed that a single use of ASKP1240 in both the induction (6-week) and maintenance (6-month) therapy markedly prolonged renal allograft survival in cynomolgus monkeys without causing apparent side effects (11,12). In particular, ASKP1240 maintenance treatment at 10 mg/kg completely suppressed both donor-specific antibody (DSA) and anti-drug antibody (ADA) formation (12). Although ASKP1240 ameliorated alloimmune responses and allowed prolongation of kidney allograft survival in NHPs, donor-specific tolerance was not achieved by the treatment, and these allografts underwent chronic allograft nephropathy (11,12).

In our previous studies, we showed that inhibition of the CD40–CD154 signaling pathway by the CD40Ig-encoded adenovirus vector allowed long-term acceptance of both liver and heart allografts in rats (13,14). Histopathology revealed that these cardiac allografts presented signs of cardiac allograft vasculopathy, whereas the hepatic allografts were normal. Furthermore, a skin-challenging test at more than 100 days after transplantation confirmed that donor-specific tolerance was induced to the liver allografts, but not to the cardiac allografts (13,14). A similar result concerning the tolerogenic effect of the CD40–CD154 signaling blockade on hepatic (15)—but not cardiac (16,17)—allografts has been shown by other researchers in rat transplantation models.

Here, we tested our hypothesis that the blockade of CD40–CD154 pathway by ASKP1240 leads to acceptance of hepatic allografts in NHPs.

Materials and Methods

Animals

Forty-nine purpose-bred male cynomolgus monkeys (*Macaca fascicularis*) including one blood donor animal, 49–75 months old (median, 56 months) with body weights ranging from 3.8 to 6.7 kg (median, 0.9 kg), were used. Animals were maintained and operated upon at the Shin Nippon Biomedical Laboratories (SNBL, Kagoshima, Japan). The experiment protocol was approved by the Animal Care and Use Committee of the SNBL, and all procedures were performed in accordance with the standards described in the Guide for the Care and Use of Laboratory Animals from the National Institutes of Health.

Liver transplantation

One donor animal was used per recipient. Twenty-four donor/recipient pairs were selected by ABO blood-type compatibility and by one-way mixed lymphocyte reaction (MLR) assays revealing a stimulation index greater than 5. In addition, the selection of monkey pairs was based on their genetic nonidentity according to major histocompatibility complex (MHC) class II DRβ, as confirmed by a direct sequencing of the second exon of DRβ as previously described (11,12). In the donor surgery, the portal vein (PV), suprahepatic vena cava (SHVC) and infrahepatic vena cava (IHVC) were dissected out. The hepatic artery was kept in continuity with the celiac trunk and abdominal aorta up to the iliac bifurcation. Before perfusion, donor blood was collected. The liver was perfused *in situ* through the aorta using cold histidine-tryptophan-ketoglutarate solution (Odyssey Pharmaceuticals, East Hanover, NJ, USA) and collected. Recipient surgery was conducted in parallel. Before removing the native liver, the superior mesenteric artery (SMA) and, if necessary, the middle colic artery, was clamped to prevent bowel congestion. Following hepatectomy, the graft liver was placed into the right hepatic fossa, and the SHVC and PV were anastomosed to those of the graft. The SMA was declamped, and, subsequently, the graft was reperfused. After completion of the IHVC anastomosis, the graft aorta conduit was finally anastomosed to the recipient aorta in an end-to-side fashion. For biliary reconstruction, cholecystoduodenostomy (18) was performed. In 2 cases (animals #23, #24), a side-to-side choledochocholedochostomy (19) was used. Animals were administered cefazolin (10 mg/kg; Astellas Pharma, Tokyo, Japan) before and after liver transplantation (LTx) for 3 days. Intravenous fluid was given for 3 days, until oral intake became adequate. Vital signs, appetite and attitude of LTx animals were mon-

itored daily. Animals were euthanized when exhibiting severe weakness, weight loss or abnormal behavior, as determined by veterinary staff and investigators.

Experimental groups and treatment protocols

The animals were randomly divided into three groups. Three animals receiving no treatment served as a control (n = 3). For the induction treatment group (n = 4), ASKP1240 (10 mg/kg) was given intravenously on days 0, 4, 7, 11 and 14. For the maintenance treatment group (n = 7), a weekly ASKP1240 (5 mg/kg) administration was subsequently continued for up to 6 months. No additional therapy was given to prevent rejection. Transplant recipients that died within 48 h after transplantation, nine due to a severe ischemia reperfusion injury (IRI) and one due to bleeding, were excluded.

Biochemical and immunological analyses

Hematology and blood chemistry: Laboratory assessments were performed three times per week for the first two postoperative weeks and weekly thereafter. Peripheral blood hematology—including red blood cell (RBC) and white blood cell (WBC) counts, hemoglobin, hematocrit and PLT counts—was performed with the ADVIA120 (Bayer Diagnostics, Sudbury, UK). The serum levels of total protein, albumin, alanine aminotransferase (ALT), aspartate aminotransferase (AST), total bilirubin (T-Bil), gamma-glutamyl transpeptidase (γ-GTP), total cholesterol, high-density lipoprotein cholesterol, creatinine, blood urea nitrogen and electrolytes were measured using the JCA-BM8 (Nippon Denshi, Tokyo, Japan).

Serum ASKP1240 trough level: For the pharmacokinetic monitoring of ASKP1240, peripheral blood samples were obtained immediately before drug administration. Serum ASKP1240 trough levels were measured using an enzyme-linked immunosorbent assay as described previously (11,12).

Donor-specific antibody (DSA): DSA was assessed by incubating the donor splenocytes with serum obtained from transplanted recipients as described previously (11,12).

Anti-ASKP1240 antibody: Anti-drug antibody (ADA) was examined by applying surface plasmon resonance technology as described previously (11,12).

Mixed lymphocyte reaction (MLR): One-way mixed lymphocyte reaction was performed before transplantation and periodically after grafting. Gamma-irradiated (30 Gy) peripheral blood mononuclear cells (PBMCs) of donor animals were used as stimulator cells, and responder PBMCs were obtained from recipient animals as described previously (11,12).

ImmuKnow: Anticoagulated whole blood was diluted with sample agent and incubated for 15–18 h with phytohemagglutinin (PHA). The following day, CD4+ T cells were positively selected with magnetic particles coated with antihuman CD4 monoclonal antibodies (Dynabeads, Oslo, Norway), washed to remove residual cells, and lysed to release intracellular adenosine triphosphate (ATP). Released ATP was measured using luciferin/luciferase and a luminometer (Turner Biosystems, Madison, WI, USA). The procedure was performed according to the manufacturer's instructions.

ELIspot: The frequencies of donor-reactive interferon (IFN)-γ–secreting T cells in the periphery were determined by the ELIspot^PLUS Monkey IFN-γ kit (Mabtech, Cleveland, OH, USA). PHA or gamma-irradiated (30 Gy) splenocytes of donor and third-party animals were used as stimulators. For the direct-response assay, the recipient's PBMCs (5 × 10^5/well) were cocultured with stimulators (1 × 10^6/well) for 24 h. For the indirect-response assay, the recipient's PBMCs (5 × 10^5/well) were cocultured with lysed

stimulator splenocytes (1 × 10⁶/well) for 40 h. ELIspot plates were pre-coated with IFN-γ capture antibody (GZ-4) for 16 h and blocked with FBS-supplemented RPMI 1640 medium for 30 min. After incubation, the plates were washed, and biotin-conjugated anti–IFN-γ Ab (7-B6-1) was added. After 2 h, the plates were incubated with streptavidin-HRP for 1 h. Spots were developed using TMB solution and were counted by computer-assisted KS ELISPOT 4.1 Software (Carl Zeiss, Thornwood, NY, USA).

Leukocyte phenotype: PBMCs were labeled with the following mAbs: CD4 (L200), CD8 (RPA-T8), CD25 (M-A251), CD28 (CD28.2), CD95 (DX-5), CD154 (TRAP1) (all from BD Biosciences Pharmingen, Mountain View, CA, USA) and FoxP3 (PCH101; eBioscience, San Diego, CA, USA) and were assessed by flow cytometry. Phenotypic surface markers for effector memory (CD28⁻CD95⁺), central memory (CD28⁺CD95⁺) and naive (CD95⁻) T cells were assessed according to the methods reported by Pitcher et al. (20) and Koyama et al. (21). Staining was performed according to the manufacturer's instructions.

Gene expression: Total RNAs were extracted from biopsy-obtained graft tissues by the RNeasy kit (QIAGEN, CA, USA) and from PBMCs by the TRIzol reagent and PureLink RNA Mini Kit (Invitrogen, Carlsbad, CA, USA). Complementary DNA was then synthesized. Oligonucleotide primers and TaqMan probes for measurement of mRNA expression of FoxP3, IL-10, TGF-β and GAPDH were designed with the Primer express software (Applied Biosystems, Foster City, CA, USA). A ready-made primer and probe kit, TaqMan Gene Expression Assays for Rhesus Macaque (Applied Biosystems), was used for measurement of IL-15 (Assay ID; Rh02621777 m1), IFN-γ (Rh02788577 m1), Perforin (Rh02621761 m1) and Granzyme B (Rh02621701 m1). PCR analysis was performed with the ABI PRISM 7900HT Fast Real-Time PCR System (Applied Biosystems). The relative mRNA expression levels in 2 μg of total RNA were calculated using the standard curve and were normalized by the GAPDH levels.

Histopathological determinations

Histological study: Liver biopsies were performed monthly after transplantation, using a 16-gauge Biopsy-Cut needle (C.R. Bard, Covington, GA, USA). Allograft rejection was evaluated histopathologically according to the Banff classification method (22). Necropsy was performed immediately after euthanization to evaluate the graft and extrahepatic organs, including the brain, lung, heart, thymus, gallbladder, spleen, pancreas, stomach, duodenum, jejunum, ileum, colon, rectum, kidney, ureter, bladder and lymph nodes. Tissue samples were fixed in 10% neutral buffered formalin, embedded in paraffin, and stained with hematoxylin and eosin. In addition, graft tissues were stained with cytokeratin 7, α-smooth muscle actin and Masson trichrome. Histopathological examination was performed by two pathologists who were not aware of the nature of the treatment group or the clinical findings.

Immunohistochemistry: Frozen tissue sections (4 μm) were fixed with cold acetone and stained by an indirect immunofluorescence technique using antihuman C4d mAb (Quidel, San Diego, CA, USA) and fluorescein isothiocyanate-conjugated rabbit antimouse IgG polyclonal antibody (Zymed, South San Francisco, CA, USA). For detection of regulatory T cells in grafts, double staining with Texas Red-conjugated rabbit polyclonal anti-FoxP3 antibody (Abcam, Cambridge, UK) and fluorescein isothiocyanate-conjugated anti-CD4 mAb (BD Biosciences, San Jose, CA, USA) was performed in the frozen sections.

Statistical analysis

All values are represented as mean (SD). An intergroup statistical analysis was performed using the Mann–Whitney U-test. The differences were considered statistically significant when a p-value was less than 0.05.
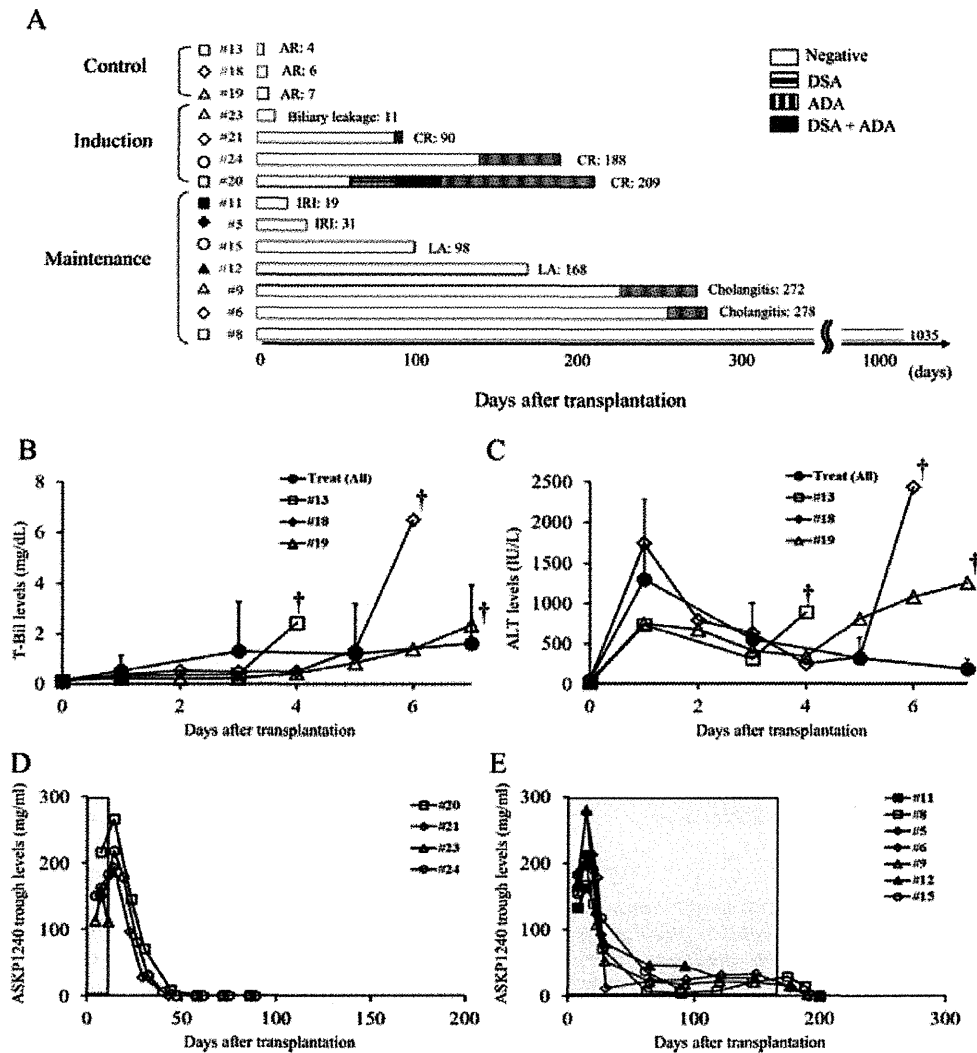
Results

Animal survival and clinical course

Allograft survival, development of DSA and ADA and final causes of death are summarized in Figure 1A. Under the standard LTx technique without using veno-veno bypass, transplant recipients died during or just after operation mainly due to the circulatory and respiratory failure without signs of rejection because this monkey was very susceptible to IRI. To overcome this, we adopted the SMA clamping technique (manuscript in preparation). Without immunosuppression, the control allografts were promptly rejected by acute cellular rejection within a week (Figure 1A). Serum T-Bil (Figure 1B) and ALT (Figure 1C) levels were exacerbated soon after LTx. The ASKP1240 induction treatment prolonged hepatic allograft survival to 90, 188 and 209 days, except for one animal that died of a biliary complication; however, these allografts were rejected by chronic rejection (Figure 1A). Serum ASKP1240 trough levels declined slowly after cessation of ASKP1240 and became undetectable at 2 months after LTx (Figure 1D). From this point, serum T-Bil levels began to increase (Figure 1F), whereas ALT levels were unstable (Figure 1H). In contrast, maintenance ASKP1240 treatment markedly prolonged liver allograft survival to 272, 278 and 1035 days (Figure 1A). The animal who survived for more than 1000 days was euthanized at day 1035 without signs of rejection. The other two of three long-term survivors were lost due to repeated cholangitis (Figure 1A) as determined by clinical course, data and histopathology. In these animals, WBC elevated along with increased differential leucocyte count during cholangitis, and by fasting and administration of antibiotics, laboratory data recovered. Another two animals were lost because of abscess formation (Figure 1A) despite treatment of cholangitis, and the other two grafts failed shortly after LTx because of a severe IRI (Figure 1A). These four grafts failed without apparent sign of acute cellular rejection. During the ASKP1240 treatment course, serum ASKP1240 trough levels were maintained for up to 200 days after LTx (Figure 1E). Within this period, serum T-Bil (Figure 1G) and ALT (Figure 1I) levels did not rise, except in some cases that experienced transient cholangitis. No serious side-effects, including thromboemboli, were observed in the animals receiving ASKP1240 treatment.

Hematology

No significant changes in RBC, WBC and PLT counts were noted in the animals, except for two cases in the maintenance treatment group that experienced spur cell anemia mainly due to liver dysfunction after LTx. This anemia, however, gradually normalized along with recovery of liver function during the ASKP1240 treatment period. Gross peripheral lymphopenia was not significant (Figures 2A and B), although absolute numbers of CD4⁺ (Figures 2C and D) and CD8⁺ (Figures 2E and F) T cells and the non–T-cell population (Figures 2G and H) in the periphery decreased

Figure 1: Clinical courses and histopathological findings in grafts of individual transplanted monkeys. (A) Results of histopathological examination showing allograft survival, treatment and cause of death. The horizontal bars represent the duration of survival of each animal after liver transplantation (LTx). The graft survival time and final diagnosis are shown at the end of the survival bar. The course of death was determined by periodical biopsy, necropsy, and clinical findings (AR, acute cellular rejection; CR, chronic rejection; IRI, ischemia reperfusion injury; LA, liver abscess). The bars also show the presence of serum donor-specific antibody (DSA) (vertical line), antidrug antibody (ADA) (cross line) or both (black fill). In the figure, #13 (open square), #18 (open diamond) and #19 (open triangle) represent the nontreated animals; #20 (open square), #21 (open diamond), #23 (open triangle) and #24 (open circle) represent the induction-treated animals and #11 (closed square), #8 (open square), #5 (closed diamond), #6 (open diamond), #12 (closed triangle), #9 (open triangle), and #15 (open circle) represent the maintenance-treated animals. The control animals (#13, #18, and #19) died shortly after LTx because of AR. The ASKP1240 induction treatment prolonged allograft survival to 90 (#21), 188 (#24) and 209 (#20) days; 1 animal died on day 11 because of biliary leakage (#23). In the ASKP1240 maintenance treatment group, 2 grafts failed at 19 (#11) and 31 (#5) days because of severe IRI, and another 2 animals died at 98 (#15) and 168 (#12) days because of LA, without signs of rejection. The other 3 animals survived for 272 (#9), 278 (#6) and 1035 (#8) days without apparent rejection. The serum ASKP1240 trough levels and both serum total bilirubin (T-Bil) and aspartate aminotransferase (AST) levels were periodically assessed before and after LTx. The shaded areas are the periods of ASKP1240 administration. Within a week after LTx, the control animals showed exacerbated serum T-Bil (B) and alanine aminotransferase (ALT) (C) levels compared with the average levels in the ASKP1240-treated animals (closed circle with error bars). The changes in ASKP1240 trough (D and E), T-Bil (F and G) and ALT (H and I) levels in the induction (D, F and H) and maintenance (E, G and I) treatment groups are shown.
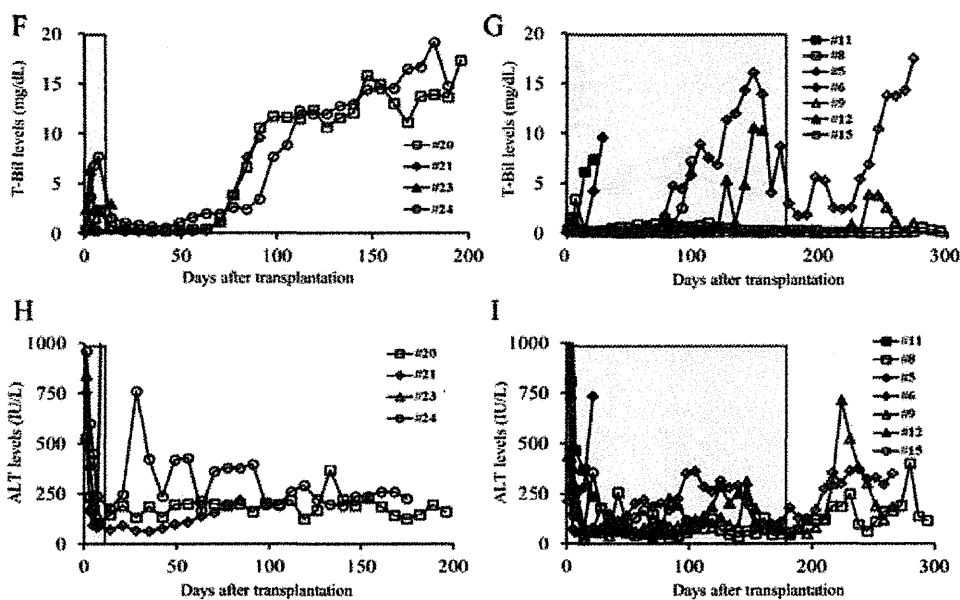
Figure 1: Continued

during ASKP1240 administration. The reduction of these lymphocytes was approximately proportional to the given dose of ASKP1240: a robust decrease within the first 2 weeks and a trend to recover slowly thereafter. However, we do not deny other possibilities for the change of lymphocyte counts such as surgery or cholangitis. The numbers of these cells recovered when ASKP1240 treatment was discontinued.

Histopathology

The failed grafts in the control group exhibited typical histopathological features of acute cellular rejection. Severe periportal lymphocyte infiltration (Figure 3A) and bile duct inflammation were observed, along with severe central venous endotheliitis (Figure 3B) and perivenular hepatocyte necrosis. In all transplanted animals treated with ASKP1240, there were, to a varying degree, pathological hallmarks of IRI and cholangitis including bile duct injury and portal fibrosis in their liver graft. In the induction treatment group, all the allografts were rejected by chronic rejection, except for one animal that had biliary leakage (Figure 1A). Histopathology revealed that periportal cellular infiltration (Figure 3C) and bile duct atrophy were observed without ductular reaction. Later, the central veins showed veno-occlusive changes (Figure 3D). In the maintenance treatment group, the allografts suffered from a severe IRI and repeated cholangitis; however, they manifested no signs of either acute or chronic rejection. Some grafts showed a slight fibrotic change in the portal tract, without persistent cellular infiltration, even after discontinuation of the maintenance ASKP1240 therapy. Although ductular reaction was observed, bile duct loss did not oc-

cur (Figure 3E). Two animals died due to IRI. Histopathology of grafts, obtained from these animals at the time of necropsy, revealed a severe dropout of hepatocytes in the perivenular area along with only a minimal cell infiltrate in the portal tract but there was no sign of acute cellular rejection. Hepatic allografts of animals euthanized at PODs 272 and 278 revealed that there were bile duct damages including ductular reaction and bridging fibrosis in the portal area, but again, without a sign of either acute or chronic rejection. A long-surviving allograft recovered at 1035 days after LTx did not show any signs of rejection; fibrotic change in the portal tract was minimal (Figures 3F–H). Microscopic abnormalities were not found in the extrahepatic organs, including the spleen, which was intact (data not shown).

Immunological studies

IFN-γ–secreting alloreactive T cells (ELIspot Assay):

During ASKP1240 treatment, both direct and indirect anti-donor cellular responses, as assessed by the frequency of IFN-γ–secreting alloreactive T cells in the periphery, were completely abolished. However, after ASKP1240 cessation, these alloreactive T cells increased in the induction therapy group (Figure 4A), whereas this was not the case following maintained ASKP1240 treatment even after ASKP1240 cessation (Figure 4B). In the longest surviving animal (#8), direct and indirect responses against donor antigens were suppressed, whereas those against third party antigens or mitogens were intact (Figure 4C).

Memory cells:
The number of peripheral CD4$^+$ and CD8$^+$ effector memory T cells (T$_{EM}$: CD28$^-$CD95$^+$) had declined at 1 month after LTx (Figures 4D and E). The T$_{EM}$,
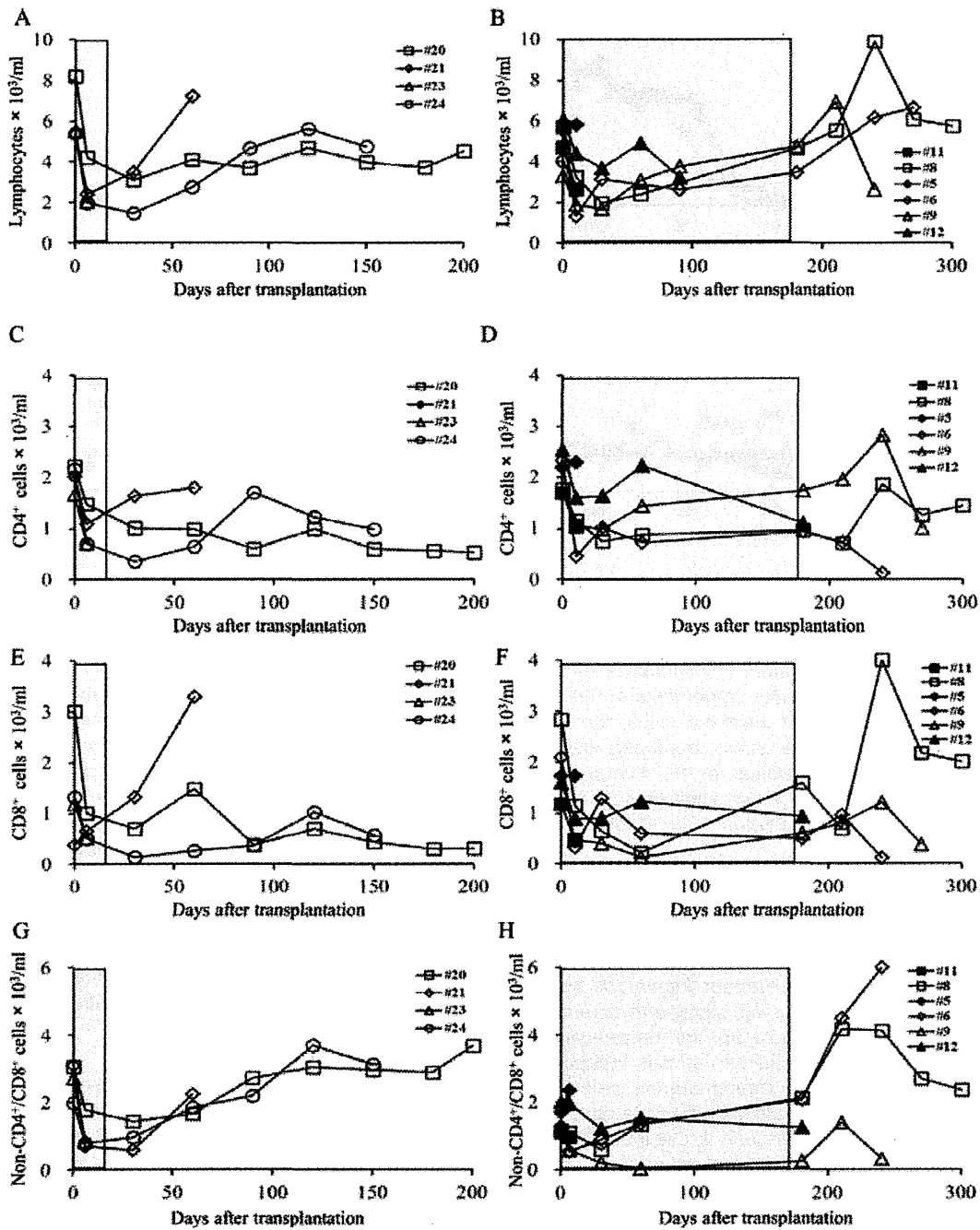
Figure 2: Changes in peripheral lymphocyte counts following induction and maintenance treatments. The counts of peripheral total (A and B), CD4+ (C and D), CD8+ (E and F) and non-CD4+/CD8+ (G and H) lymphocytes following induction (A, C, E and G) and maintenance (B, D, F and H) ASKP1240 treatment are presented. In the figure, #20 (open square), #21 (open diamond), #23 (open triangle) and #24 (open circle) have been used to represent the induction-treated animals, and #11 (closed square), #8 (open square), #5 (closed diamond), #6 (open diamond), #12 (closed triangle) and #9 (open triangle) have been used to represent the maintenance-treated animals. The shaded areas are periods of ASKP1240 administration. The peripheral lymphocyte counts decreased to values ranging from one-third to two-thirds of the preoperative value within 50 days after LTx. In the ASKP1240 induction treatment group, peripheral lymphocyte counts recovered gradually after cessation of treatment. In the maintenance treatment group, although the same tendency was observed shortly after LTx, lymphocyte count recovery was noted during the ASKP1240 treatment course.
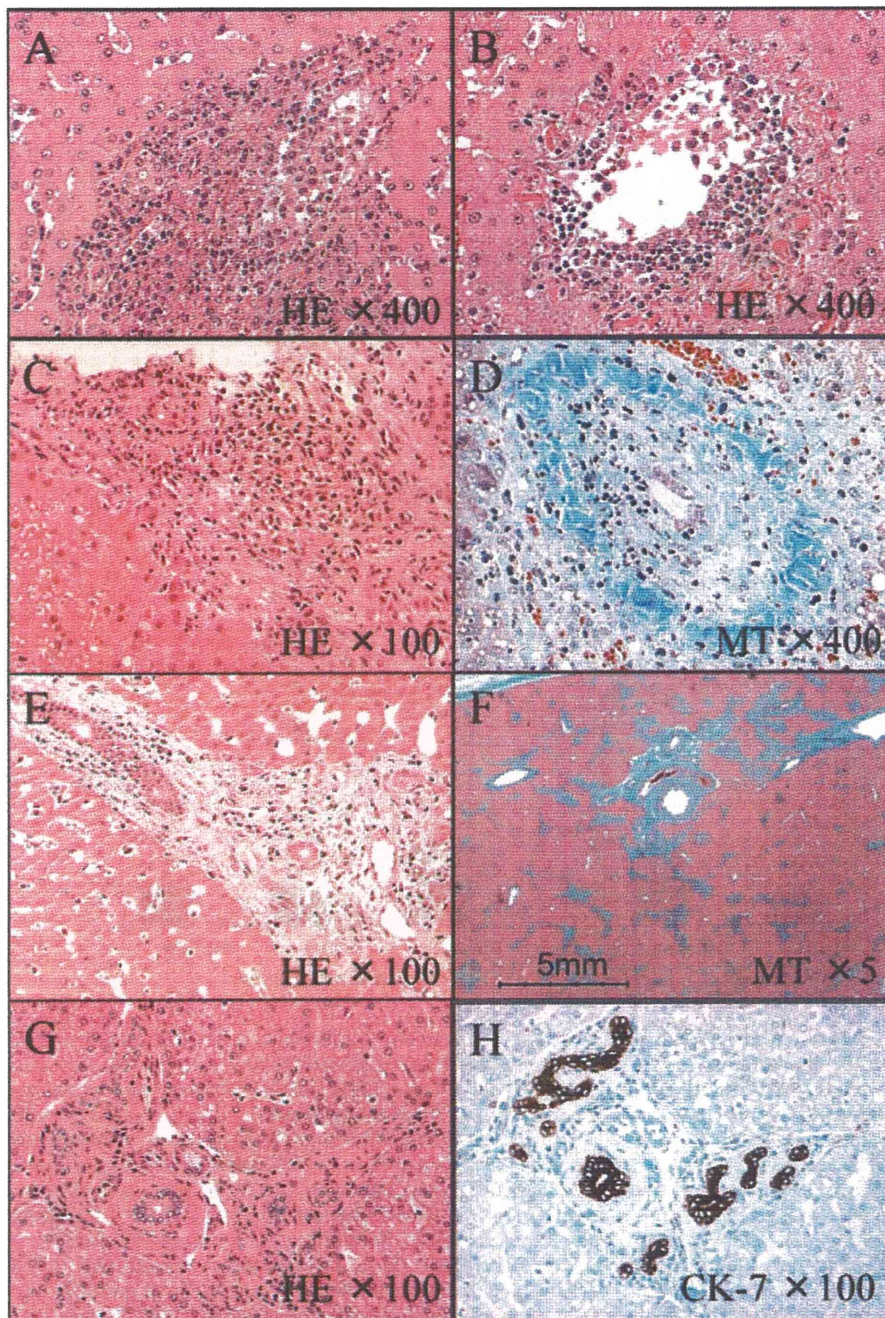
Figure 3: Histopathology of hepatic allografts. Microscopic appearance of liver allografts from the control (A, B), induction treatment (C, D) and maintenance treatment (E–H) groups. The control allograft at postoperative day (POD) 4 (#13) manifested acute cellular rejection with severe leukocyte infiltration in the periportal area (A), bile duct and central vein (B). Hepatic allografts, obtained from the induction treatment group at POD 88 (#24: C) and POD 209 (#20: D), manifested chronic rejection with mild periportal cell infiltration (C), bile duct atrophy and loss and veno-occlusive changes (D). Graft liver excised at POD 174 (#9: E) and POD 1035 (#8: F, G and H) from the ASKP1240 maintenance treatment group manifested no signs of acute cellular or chronic rejection. The portal tract showed mild fibrotic change and edema with minimal inflammation and eosinophilic infiltration (E). A ductular reaction was observed without bile duct loss. Minimal portal fibrosis and ductular reaction in the central vein was noted without apparent fibrosis. A long-term surviving liver graft showed occasional bridging portal fibrosis (F) and portal fibrosis with minimal inflammatory cell infiltration with good interlobular bile duct preservation (G), and with ductular proliferation (H). (HE, hematoxylin–eosin stain; CK-7, cytokeratin-7 stain; MT, Masson trichrome stain.)

particularly CD4$^+$ cells, significantly increased after the termination of ASKP1240-induction therapy (Figure 4D), whereas they did not rise at all when ASKP1240 was maintained (Figure 4E). A similar trend was observed in changes of CD8$^+$ T$_{EM}$ (Figures 4D and E).

Antigen-specific CD4$^+$CD154$^+$ cells: Recently, it has been shown that *de novo* CD154 expression on CD4$^+$ T cells after stimulation identifies antigen-specific (23, 24) and also alloantigen-specific (25) phenotypes. Thus, we examined this population in the periphery. In the untreated control animals, the number of CD4$^+$CD154$^+$ T cells responding to the donor antigens increased, whereas the ASKP1240 treatment abrogated the elevation of this CD4$^+$CD154$^+$ T-cell population even after drug cessation in both the induction and maintenance treatment groups (Figure 4F).
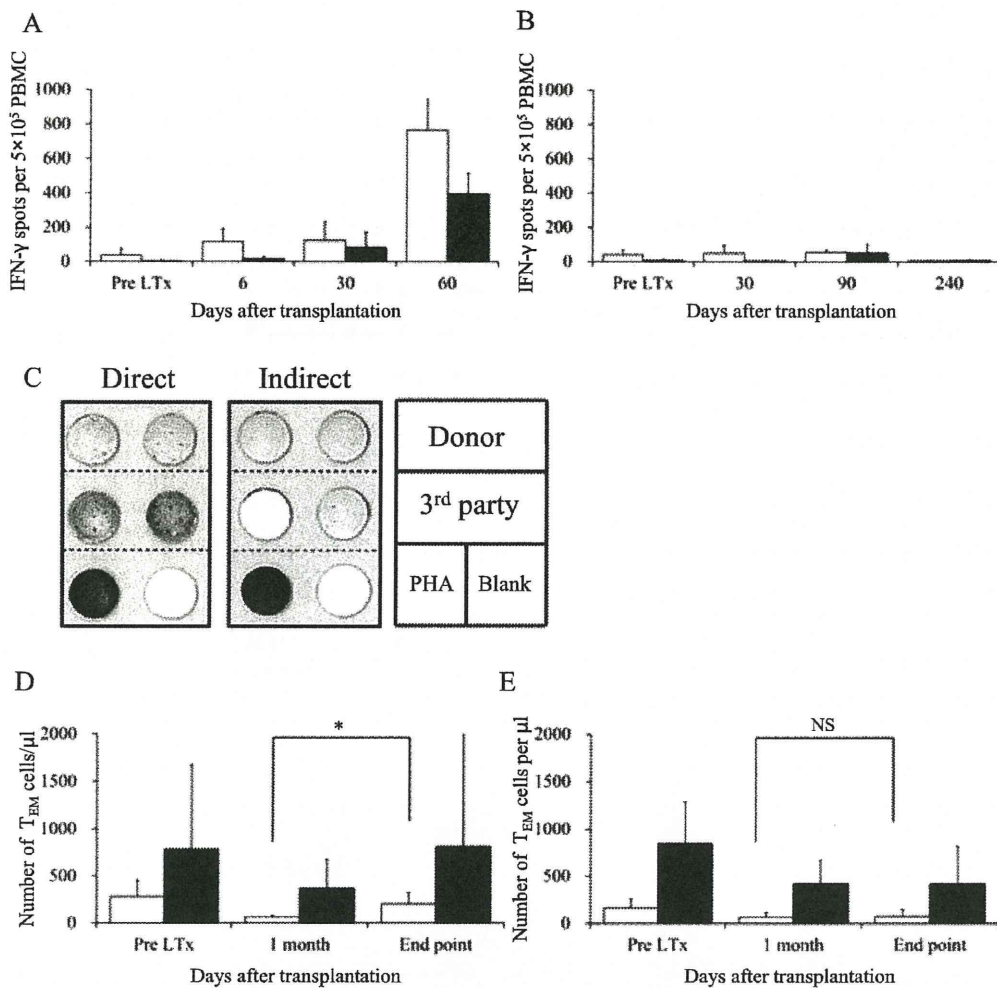
Figure 4: Cellular alloimmune responses to hepatic allografts. The frequencies of directly and indirectly stimulated, donor-reactive IFN-γ –secreting T cells in the induction (A) and maintenance (B) treatment groups were evaluated with ELIspot assay. White and black vertical bars represent the directly and indirectly stimulated IFN-γ spots, respectively. In the ASKP1240 induction treatment group, the frequencies of donor-reactive T cells in the periphery increased after drug cessation (A), whereas alloreactive T cells responding through direct and indirect pathways did not increase even after drug cessation in the ASKP1240 maintenance treatment group (B). In the longest surviving animal (#8), the frequencies of donor-reactive IFN-γ –producing cells were still minimal at day 389, although responses against third-party antigens and phytohemagglutinin (PHA) were maintained (C). The number of peripheral T_{EM} (CD28$^-$CD95$^+$) cells following induction (D) and maintenance (E) treatment was examined. The white and black vertical bars indicate cell counts of CD4$^+$ and CD8$^+$ T_{EM}, respectively. The terminal end point was defined at 12 months after LTx or just before death if the animal did not survive for >12 months. In the ASKP1240 induction treatment group (D), the numbers of circulating CD4$^+$ T_{EM} cells significantly increased after LTx. A similar trend was observed for the generation of CD8$^+$ T_{EM} cells. In the ASKP1240 maintenance treatment group (E), neither CD4$^+$ nor CD8$^+$ T_{EM} cells increased, even after drug cessation. Dot plots show that the proportion of donor-specific CD4$^+$CD154$^+$ T cells in the control allografts was higher than those of the naive and ASKP1240-treated allografts (F). The individual ATP values are presented in the induction (G) and maintenance (H) treatments. In the figure, #20 (open square), #21 (open diamond), #23 (open triangle) and #24 (open circle) represent the induction-treated animals, and #11 (closed square), #8 (open square), #5 (closed diamond), #6 (open diamond), #12 (closed triangle) and #9 (open triangle) represent the maintenance-treated animals. † and ∗ indicate chronic rejection (G) and cholangitis (H), respectively. ImmuKnow ATP values were not affected by either rejection or infection episodes (G and H). The shaded areas are periods of ASKP1240 administration (*p < 0.05, Mann–Whitney U-test; NS, not significant).
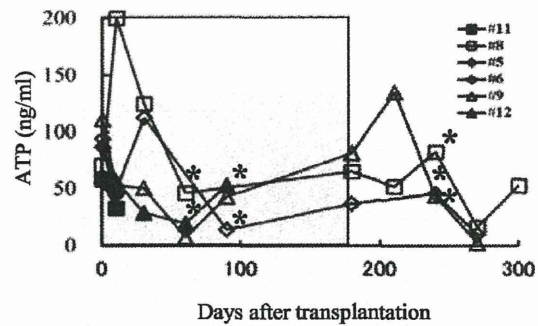
F

G

Days after transplantation

H

Days after transplantation
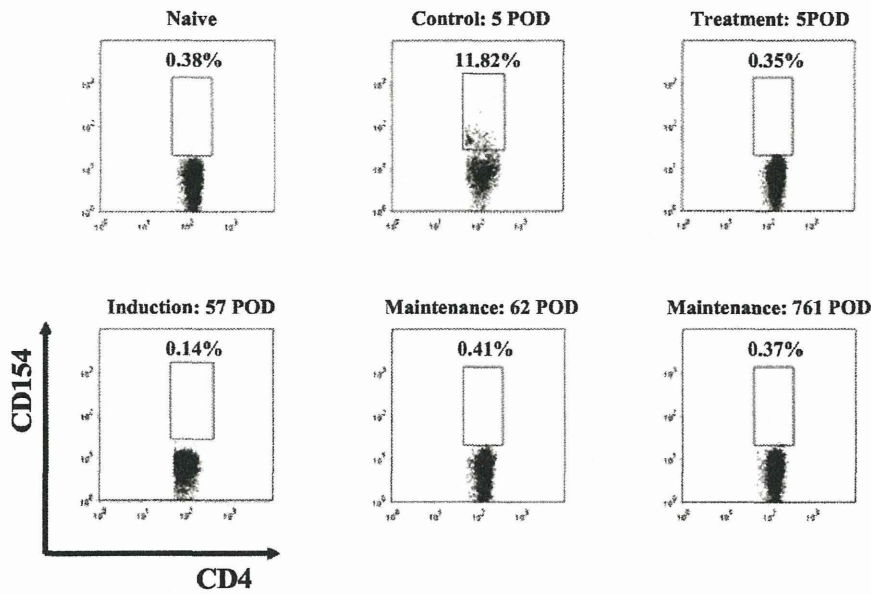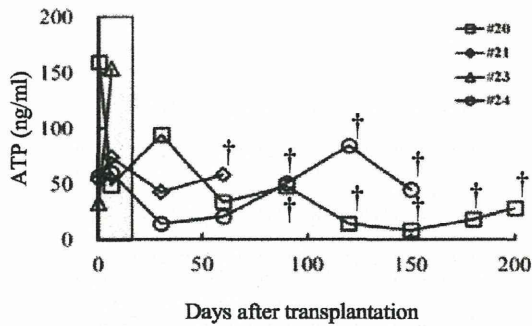
Figure 4: Continued

ImmuKnow ATP values: In all groups, the Immu-Know ATP values (ng/mL) were not affected by either rejection or infection throughout the course of the study (Figures 4G and H).

DSA and ADA formation: Formation of antidonor IgM and IgG antibodies in sera was suppressed during the treatment course, whereas they tended to rise after ASKP1240 cessation in both the induction and maintenance treatment groups (Figures 1A and 5A–D). Both the induction and maintenance ASKP1240 treatments completely suppressed anti-ASKP1240 antibody formation (Figure 1A), except for 1 animal (#20) that experienced a transient increase after drug cessation.

Immunohistochemistry: Neither C4d nor IgG deposition was observed in the allografts that underwent chronic rejection or survived without a sign of rejection (Figures 5E and F). The proportion of Foxp3^{+} cells in the long-term surviving allografts did not rise at all as compared with those of the rejected allografts (data not shown).

Regulatory T cells (T_{reg}): The peripheral CD4^{+} CD25^{+}Foxp3^{+} regulatory T-cell subset did not increase, even in the long-term surviving animals without rejection. Rather, a higher proportion of this subset was observed in animals that rejected allografts by acute cellular rejection (Figure 6A). At early a time point after LTx, T_{EM}/T_{reg} ratio of the ASKP1240-treated animals was low. After the
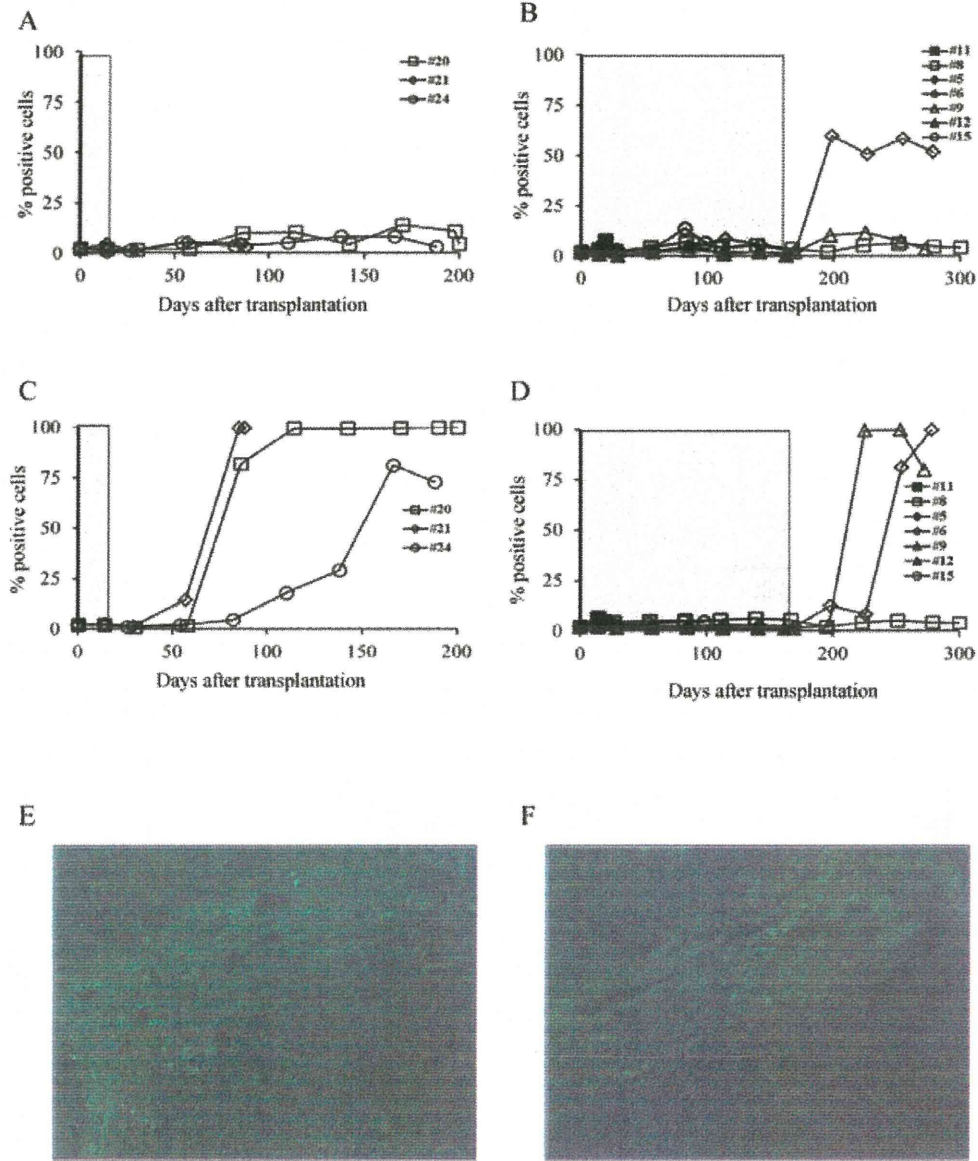
Figure 5: Humoral immune responses to hepatic allografts. The formation of antidonor IgM (A and B) and IgG (C and D) antibodies in sera following ASKP1240 induction (A and C) and maintenance (B and D) treatment was monitored by flow cytometric analysis. In the figure, #20 (open square), #21 (open diamond) and #24 (open circle) represent the induction-treated animals, and #11 (closed square), #8 (open square), #5 (closed diamond), #6 (open diamond), #12 (closed triangle), #9 (open triangle) and #15 (open circle) represent the maintenance-treated animals. The shaded areas are periods of ASKP1240 administration. During the ASKP1240 treatment period, antidonor antibodies were not detected. After cessation of ASKP1240 treatment, the serum antidonor IgG level increased. No allografts showed deposition of C4d (E) or IgG (F) (#8; POD 445).

drug cessation, this ratio significantly increased in both the induction and maintenance treatment groups; however, elevation of T_{EM}/T_{reg} ratio was significantly higher in the induction-treated animals as compared to that of maintenance-treated ones (Figure 6B). Intragraft Foxp3 expression, as detected by immunohistochemistry (data not

shown) and PCR (Figure 6C), did not show any significant change by the ASKP1240 treatment in the transplanted animals.

PCR: The intragraft Granzyme B mRNA expression level (Figure 6D) was significantly down-regulated in the animals
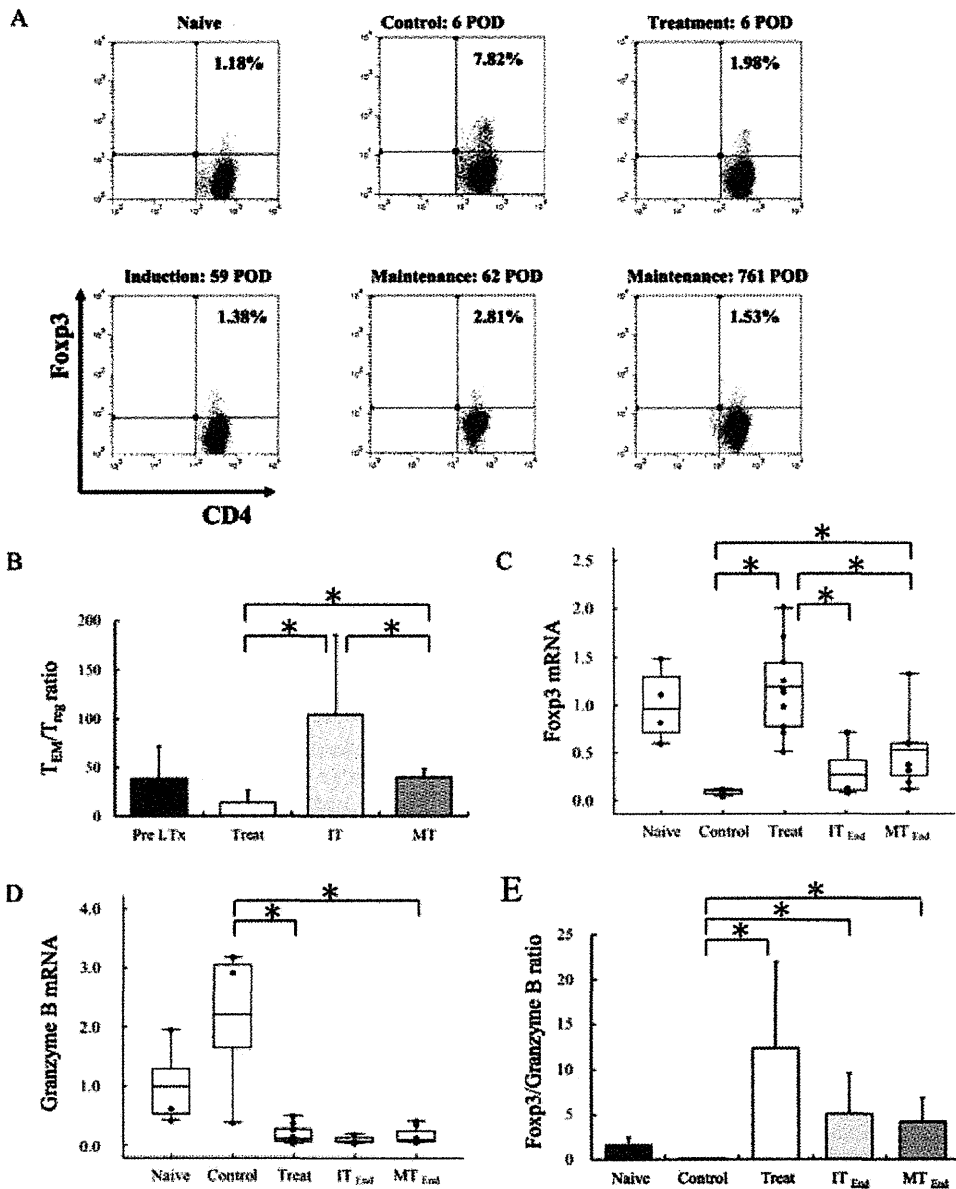
Figure 6: T_reg population in the periphery and graft and expression of intragraft gene transcripts. (A) The CD4+Foxp3+ T-cell population in the periphery was assessed by flow cytometry, and representative dot-plot analyses data are shown. The CD4+Foxp3+ T cells did not increase at all, except in animals that did not receive ASKP1240 treatment and acutely rejected the liver allograft. (B) The T_{EM}/T_{reg} ratio was examined before and after ASKP1240 treatment. Results at before LTx (Pre-LTx, n = 10), at POD 10 (Treat, n = 10), at 1 month after LTx with induction treatment (IT, n = 3) and at 8 months after LTx with maintenance treatment (MT, n = 3) are shown. After drug cessation, the T_{EM}/T_{reg} ratio was significantly increased. A significant difference was observed between the induction and maintenance treatments. The expression levels of Foxp3 (C) and Granzyme B (D) were assessed by real-time polymerase chain reaction (RT-PCR) in the liver specimens. Tissue samples were obtained from naive monkeys (Naïve, n = 4), untreated control allografts at the time of necropsy (Control, n = 3), all of the ASKP1240-treated animals at POD 10 (Treat, n = 10), and animals given the induction (IT_End, n = 3) and maintenance (MT_End, n = 7) ASKP1240 treatments at the end time point. The end point is defined as the time of necropsy. Each transcript was normalized by glyceraldehyde-3-phosphate dehydrogenase (GAPDH). The results are given as fold-change differences with respect to that of naive monkeys, and presented as whisker plots for the 25th and 75th percentiles, mean and maximum and minimum values with individual data. No upregulation of Foxp3 transcript was observed, in even the long-term surviving animals compared with the animals during ASKP1240 administration (C). The intragraft expression level of Granzyme B increased in the control group, whereas the Granzyme B level was suppressed by ASKP1240 treatment (D). The Foxp3/Granzyme B ratio was significantly increased by ASPK1240 treatment (E) (*$p < 0.05$, Mann–Whitney U-test).

during treated and maintained, whereas the levels of Foxp3 (Figure 6C), TGF-β, IL-10, Perforin, IL-15 and IFN-γ (data not shown) transcripts did not correspond to freedom from graft rejection. ASKP1240 treatment significantly increased the Foxp3/Granzyme B ratio as compared with that of the nontreated control (Figure 6E).

Discussion

In this study, we have shown that a novel fully human anti-CD40 mAb, ASKP1240, markedly prolonged hepatic allograft survival in NHPs. According to the findings of our previous dose-dependent study on kidney transplantation (12), we adopted the induction and maintenance treatment protocols using ASKP1240 at a dose of 10 mg/kg. In contrast to renal allografts, the maintenance ASKP1240 treatment prevented rejection for the duration of therapy, and in one animal resulted in a long-term hepatic allograft acceptance. However, the induction ASKP1240 therapy resulted in graft chronic rejection after drug cessation. Prevention of allograft rejection with the maintenance-ASKP1240 treatment was associated with a potent suppression of both the direct and indirect cellular alloimmune responses, as assessed by the IFN-γ ELIspot assay. Furthermore, we found that the direct and indirect responses against third party or PHA antigens remained intact in the long-term survivors. These results were in contrast to the induction ASKP1240 treatment, which permitted recovery of both direct and indirect alloimmune responses after termination of ASKP1240 treatment. Hering et al. (26) demonstrated a marked suppression of IFN-γ –secreting donor-reactive T cells via the indirect pathway in recipient monkeys who had accepted porcine islet xenografts for over 100 days by using multiple immunosuppressants, including the anti-CD40L mAb.

The existence of memory T cells, which are resistant to various immunosuppressants (including costimulation blockers), has been regarded as a major barrier to the induction of transplantation tolerance (27). Weaver et al. (28) showed that elimination of memory T cells by combined LFA-3-Ig and CTLA4-Ig treatment contributed to kidney allograft acceptance in NHPs. Although the peripheral T_{EM} population increased shortly after termination of the induction ASKP1240 treatment, the T_{EM} cells were completely abolished by the maintenance ASKP1240 therapy, even after drug cessation. Along with suppression of cellular responses through the direct and indirect pathways, inhibition of T_{EM} cells seems to contribute to the ASKP1240 treatment's effect on the prevention of allograft rejection.

Previous studies have demonstrated that inhibition of the CD40–CD154 signaling pathway induces regulatory T cells (T_{reg}) (29) and that higher T_{reg} expression in the periphery is associated with an operational tolerance in a clinical LTx setting (30). We therefore assessed whether ASKP1240

treatment induced an immunoregulatory mechanism. In the results of our FACS and RT-PCR analyses, however, there was no clear evidence of T_{reg} induction by ASKP1240 administration. During the treatment period, the T_{EM}/T_{reg} ratio was suppressed; however, after drug cessation this ratio significantly increased, especially in the induction-treated animals. Although an increase in the T_{reg} population in the periphery or graft liver was not evident, a significant reduction of IFN-γ producing cells, antigen-specific $CD4^+CD154^+$ T cells, and T_{EM} by ASKP1240 administration suggests a possibility that suppression of allo-aggressive T cells by the maintenance ASKP1240 treatment consequently shifted the balance toward a tolerogenic state.

In addition inhibiting cellular immune responses, ASKP1240 completely suppressed both DSA and ADA formation during the treatment course. Of the three long-term–surviving liver transplant recipients, two developed DSA after cessation of ASKP1240; however, there was no sign of antibody-mediated rejection, which was confirmed by graft C4d and IgG staining. This result was in contrast to our previous ASKP1240 trial in kidney transplantation, in which the grafts became positive to C4d and IgG and all the renal allografts underwent chronic nephropathy (12). Indeed, humoral mechanisms of alloreactivity mediated by DSA appear to frequently operate along with cellular mechanisms (31). In this study, we did not directly assess a helper T-cell function. Therefore, we do not deny the possibility that incomplete suppression of helper T cells by ASKP1240 treatment permitted formation of DSA, although there was no histopathological evidence of humoral rejection in the liver grafts. Many studies have shown that development of DSA is a major risk for chronic renal allograft rejection (32) and positive C4d graft staining is a hallmark of chronic renal allograft rejection (33). In LTx, similar findings have been reported (34,35). However, it is well known that liver allografts are resistant to HLA incompatibility or positive cross-match (36), and this unique immunoprivilege of the liver grafts (37) may have caused a discrepancy in the efficacy of ASKP1240 on different organ transplants. Although we have demonstrated that donor specific effector function was completely suppressed but the responses against third-party antigens and PHA were maintained in the long-survived animal following treatment cessation, by considering forementioned results regarding the DSA, we could not identify whether a donor-specific tolerance was induced in the maintenance ASKP1240-treated transplant recipients.

Fibrotic change of the portal tract was indicated by protocol biopsies in all grafts at 1 month after LTx. The degree of fibrosis varied and did not correspond to the type of ASKP1240 treatment protocol. Insufficient immunosuppression can be a risk factor of development of graft fibrosis and chronic rejection (38); however, this explanation seems unlikely because the fibrosis was already noted after LTx when both the cellular and humoral alloimmune

responses were abolished by ASKP1240 administration, as shown by several assays. Rather, this rapid peri-portal fibrotic change seems to be a hallmark of IRI, which has been shown previously to play a major role in graft fibrosis in the liver (39) and other organs (40). In fact, the cynomolgus monkey liver was very susceptible to ischemia: in our preliminary study, most of recipient monkeys died within 24 hours after LTx because the veno-veno bypass was not applicable in these small monkeys. Instead, we adopted a technique of clamping the SMA during an anhepatic phase (manuscript in preparation). Even using this unique technique, a severe IRI to the hepatic allograft was not completely abolished, as indicated by a considerable elevation of serum AST and ALT levels following LTx.

In the graft liver of the animals treated with a short course induction of ASKP1240, cellular infiltrates increased and the fibrotic area expanded after cessation of ASKP1240; finally, the bile ducts were microscopically lost, which indicated progression of chronic allograft rejection. In contrast, histopathological changes—including signs of neither acute nor chronic rejection—were present in the liver grafts when ASKP1240 treatment was maintained. In addition, these animals experienced repeated cholangitis that required fasting and antibiotic treatment. Two animals were eventually lost due to abscess formation. The episodes of cholangitis provoked biliary cirrhotic changes to the graft livers; persistence of fibrosis and bile duct proliferation (but not disappearance) were confirmed by histology. Indeed, similar microscopic features were reported by Gotoh et al. (41) in long-term–surviving liver grafts under FK506 treatment in cynomolgus monkeys. We used the ImmuKnow® for the purpose of assessing an immunological state, because it has been shown as an useful tool in clinical transplantation (42). In our study, however, ImmuKnow® values did not decline even when the animals suffered from cholangitis or liver abscess. We do not deny the possibility that ASKP1240 treated animals were over-immunosuppressed, especially when ASKP1240 treatment was maintained. However, the only infectious complication apparent in the treated animals was cholangitis/biloma, and we consider that this complication occurred because of the biliary reconstruction method, cholecystoduodenostomy, in the current LTx model.

As in our previous studies (11,12), ASKP1240 did not cause obvious adverse events in the treated monkey liver recipients. Of all the animals, two experienced transient anemia. In their peripheral blood smear, achantrocytes were observed, and this phenomenon was diagnosed as spur cell anemia due to liver dysfunction (43). This anemia emerged at 2–3 months after LTx, and the animals recovered gradually but spontaneously from anemia during the ASKP1240 treatment course, corresponding to the improvement of liver function. The administration of ASKP1240 reduced peripheral non-T lymphocytes and suppressed germinal center formation in the spleen and lymph nodes at the time of autopsy (data not shown). These phenomena were also noted in our earlier studies (11,12); this effect seems to be mediated via the inhibition of CD40 signaling pathway by ASKP1240, as the CD40–CD154 axis induces B-cell proliferation, antibody production, immunoglobulin isotype switching and germinal center formation (44–47).

Ligation of CD40 to CD154 on T cells plays a crucial role in cellular immunity. Signals via CD40 on dendritic cells (DCs) and monocytes engender these cells into a fully competent antigen-presenting cells (APCs), that can reciprocally trigger the cognate T cells to clonally expand and differentiate (45). Also, CD40 activation leads to cell proliferation, antibody production and immunoglobulin isotype switching in B cells that puts forward humoral immunity (44). On the basis of the role of CD40 signaling in the immunity, interruption of CD40/CD154 interaction can result in inadequate antigen presentation and a deficiency in both cellular and humoral immune responses. Indeed, in this study, we have demonstrated that inhibition of CD40 signal by ASKP1240 completely suppressed antidonor cellular responses and inhibited generation of DSA and ADA during the treatment course in the LTx recipients. Because we did not directly evaluate the effects at a cellular level in the current study, we cannot explain the exact mechanisms of immunomodulatory effect achieved by treatment with ASKP1240. Further studies are warranted to elucidate this subject.

In conclusion, a fully human anti-CD40 mAb, ASKP1240, induced potent immunosuppressive effects for hepatic allografts in NHPs without causing serious side effects. CD40 blockade by ASKP1240 ameliorates cellular and humoral alloimmune responses and prevented rejection for the duration of therapy, and in one animal resulted in a long-term acceptance in cynomolgus monkeys, especially when treatment is sustained. The present results indicate that ASKP1240 is a promising agent for immunosuppression in LTx.

Acknowledgments

Disclosure

The authors of this manuscript have no conflicts of interest to disclose as described by the *American Journal of Transplantation*.

References

1. Sayegh MH, Turka LA. The role of T-cell costimulatory activation pathways in transplant rejection. N Engl J Med 1998; 338: 1813–1821.
2. Larsen CP, Elwood ET, Alexander DZ, et al. Long-term acceptance of skin and cardiac allografts after blocking CD40 and CD28 pathways. Nature 1996; 381: 434–438.
3. Larsen CP, Alexander DZ, Hollenbaugh D, et al. CD40-gp39 interactions play a critical role during allograft rejection. Suppression of allograft rejection by blockade of the CD40-gp39 pathway. Transplantation 1996; 61: 4–9.
4. Kirk AD, Burkly LC, Batty DS, et al. Treatment with humanized monoclonal antibody against CD154 prevents acute renal allograft rejection in nonhuman primates. Nat Med 1999; 5: 686–693.
5. Preston EH, Xu H, Dhanireddy KK, et al. IDEC-131 (anti-CD154), sirolimus and donor-specific transfusion facilitate operational tolerance in non-human primates. Am J Transplant 2005; 5: 1032–1041.
6. Kanmaz T, Fechner JJ, Jr., Torrealba J, et al. Monotherapy with the novel human anti-CD154 monoclonal antibody ABI793 in rhesus monkey renal transplantation model. Transplantation 2004; 77: 914–920.
7. Kawai T, Andrews D, Colvin RB, Sachs DH, Cosimi AB. Thromboembolic complications after treatment with monoclonal antibody against CD40 ligand. Nat Med. 2000; 6: 114.
8. Andre P, Prasad KS, Denis CV, et al. CD40L stabilizes arterial thrombi by a beta3 integrin–dependent mechanism. Nat Med 2002; 8: 247–252.
9. Haanstra KG, Ringers J, Sick EA, et al. Prevention of kidney allograft rejection using anti-CD40 and anti-CD86 in primates. Transplantation 2003; 75: 637–643.
10. Pearson TC, Trambley J, Odom K, et al. Anti-CD40 therapy extends renal allograft survival in rhesus macaques. Transplantation 2002; 74: 933–940.
11. Imai A, Suzuki T, Sugitani A, et al. A novel fully human anti-CD40 monoclonal antibody, 4D11, for kidney transplantation in cynomolgus monkeys. Transplantation 2007; 84: 1020–1028.
12. Aoyagi T, Yamashita K, Suzuki T, et al. A human anti-CD40 monoclonal antibody, 4D11, for kidney transplantation in cynomolgus monkeys: Induction and maintenance therapy. Am J Transplant 2009; 9: 1732–1741.
13. Nomura M, Yamashita K, Murakami M, et al. Induction of donor-specific tolerance by adenovirus-mediated CD40Ig gene therapy in rat liver transplantation. Transplantation 2002; 73: 1403–1410.
14. Yamashita K, Masunaga T, Yanagida N, et al. Long-term acceptance of rat cardiac allografts on the basis of adenovirus mediated CD40Ig plus CTLA4Ig gene therapies. Transplantation 2003; 76: 1089–1096.
15. Chang GJ, Liu T, Feng S, et al. Targeted gene therapy with CD40Ig to induce long-term acceptance of liver allografts. Surgery 2002; 132: 149–156.
16. Guillot C, Guillonneau C, Mathieu P, et al. Prolonged blockade of CD40-CD40 ligand interactions by gene transfer of CD40Ig results in long-term heart allograft survival and donor-specific hyporesponsiveness, but does not prevent chronic rejection. J Immunol 2002; 168: 1600–1609.
17. Guillonneau C, Hill M, Hubert FX, et al. CD40Ig treatment results in allograft acceptance mediated by CD8CD45RC T cells, IFN-gamma, and indoleamine 2,3-dioxygenase. J Clin Invest 2007; 117: 1096–1106.
18. Monden M, Gotoh M, Kanai T, Valdivia LA, Umeshita K, Endoh W et al. A potent immunosuppressive effect of FK 506 in orthotopic liver transplantation in primates. Transplant Proc 1990; 22: 66–71.
19. Neuhaus P, Neuhaus R, Pichlmayr R, et al. An alternative technique of biliary reconstruction after liver transplantation. Res Exp Med (Berl) 1982; 180: 239–245.
20. Pitcher CJ, Hagen SI, Walker JM, et al. Development and homeostasis of T cell memory in rhesus macaque. J Immunol 2002; 168: 29–43.
21. Koyama I, Nadazdin O, Boskovic S, et al. Depletion of CD8 memory T cells for induction of tolerance of a previously transplanted kidney allograft. Am J Transplant 2007; 7: 1055–1061.
22. Demetris A, Adams D, Bellamy C, et al. Update of the International Banff Schema for liver allograft rejection: Working recommendations for the histopathologic staging and reporting of chronic rejection: An international panel. Hepatology 2000; 31: 792–799.
23. Frentsch M, Arbach O, Kirchhoff D, et al. Direct access to CD4+ T cells specific for defined antigens according to CD154 expression. Nat Med 2005; 11: 1118–1124.
24. Chattopadhyay PK, Yu J, Roederer M. A live-cell assay to detect antigen-specific CD4+ T cells with diverse cytokine profiles. Nat Med 2005; 11: 1113–1117.
25. Ashokkumar C, Talukdar A, Sun Q, et al. Allospecific CD154+ T cells associate with rejection risk after pediatric liver transplantation. Am J Transplant 2009; 9: 179–191.
26. Hering BJ, Wijkstrom M, Graham ML, et al. Prolonged diabetes reversal after intraportal xenotransplantation of wild-type porcine islets in immunosuppressed nonhuman primates. Nat Med 2006; 12: 301–303.
27. Valujskikh A, Li XC. Frontiers in nephrology: T cell memory as a barrier to transplant tolerance. J Am Soc Nephrol 2007; 18: 2252–2261.
28. Weaver TA, Charafeddine AH, Agarwal A, et al. Alefacept promotes co-stimulation blockade based allograft survival in nonhuman primates. Nat Med 2009; 15: 746–749.
29. Taylor PA, Friedman TM, Korngold R, et al. Tolerance induction of alloreactive T cells via ex vivo blockade of the CD40:CD40L costimulatory pathway results in the generation of a potent immune regulatory cell. Blood 2002; 99: 4601–4609.
30. Pons JA, Revilla-Nuin B, Baroja-Mazo A, et al. FoxP3 in peripheral blood is associated with operational tolerance in liver transplant patients during immunosuppression withdrawal. Transplantation 2008; 86: 1370–1378.
31. Turgeon NA, Kirk AD, Iwakoshi NN. Differential effects of donor-specific alloantibody. Transplant Rev 2009; 23: 25–33.
32. Terasaki PI. Humoral theory of transplantation. Am J Transplant 2003; 3: 665–673.
33. Mauiyyedi S, Pelle PD, Saidman S, et al. Chronic humoral rejection: Identification of antibody-mediated chronic renal allograft rejection by C4d deposits in peritubular capillaries. J Am Soc Nephrol 2001; 12: 574–582.
34. Martelius T, Halme L, Arola J, et al. Vascular deposition of complement C4d is increased in liver allografts with chronic rejection. Transpl Immunol 2009; 21: 244–246.
35. Musat AI, Agni RM, Wai PY, et al. The significance of donor-specific HLA antibodies in rejection and ductopenia development in ABO compatible liver transplantation. Am J Transplant 1111; 11: 500–510.
36. Markus BH, Duquesnoy RJ, Gordon RD, et al. Histocompatibility and liver transplant outcome. Does HLA exert a dualistic effect? Transplantation 1988; 46: 372–377.
37. Starzl TE. The "privileged" liver and hepatic tolerogenicity. Liver Transpl 2001; 7: 918–920.
38. Evans HM, Kelly DA, McKiernan PJ, et al. Progressive histological damage in liver allografts following pediatric liver transplantation. Hepatology 2006; 43: 1109–1117.

39. Cheng F, Li Y, Feng L, et al. Hepatic stellate cell activation and hepatic fibrosis induced by ischemia/reperfusion injury. Transplant Proc 2008; 40: 2167–2170.

40. Lee JK, Zaidi SH, Liu P, et al. A serine elastase inhibitor reduces inflammation and fibrosis and preserves cardiac function after experimentally-induced murine myocarditis. Nat Med 1998; 4: 1383–1391.

41. Gotoh M, Monden M, Kanai T, et al. Tolerance induction by liver grafting and FK 506 treatment in nonhuman primates. Transplant Proc 1991; 23: 3265–3268.

42. Kowalski RJ, Post DR, Mannon RB, et al. Assessing relative risks of infection and rejection: A meta-analysis using an immune function assay. Transplantation 2006; 82: 663–668.

43. Cooper RA. Hemolytic syndromes and red cell membrane abnormalities in liver disease. Semin Hematol 1980; 17: 103–112.

44. van Kooten C, Banchereau J. CD40-CD40 ligand. J Leukoc Biol 2000; 67: 2–17.

45. Quezada SA, Jarvinen LZ, Lind EF, et al. CD40/CD154 interactions at the interface of tolerance and immunity. Annu Rev Immunol 2004; 22: 307–328.

46. Foy TM, Laman JD, Ledbetter JA, et al. gp39-CD40 interactions are essential for germinal center formation and the development of B cell memory. J Exp Med 1994; 180: 157–163.

47. Kawabe T, Naka T, Yoshida K, et al. The immune responses in CD40-deficient mice: Impaired immunoglobulin class switching and germinal center formation. Immunity 1994; 1: 167–178.

Supporting Information

Additional Supporting Information may be found the online version of this article.

Figure S1: Changes in peripheral T_{EM}/T_{reg} ratio of a long-survived animal (#8).

Please note: Wiley-Blackwell is not responsible for the content or functionality of any supporting materials supplied by the authors. Any queries (other than missing material) should be directed to the corresponding author for the article.

ORIGINAL ARTICLE

Successful transplantation of rat hearts subjected to extended cold preservation with a novel preservation solution

Kenji Wakayama,[1] Moto Fukai,[1] Kenichiro Yamashita,[1] Taichi Kimura,[2] Gentaro Hirokata,[1] Susumu Shibasaki,[1] Daisuke Fukumori,[1] Sanae Haga,[3] Mitsuru Sugawara,[4] Tomomi Suzuki,[1] Masahiko Taniguchi,[1] Tsuyoshi Shimamura,[1] Hiroyuki Furukawa,[1] Michitaka Ozaki,[3] Toshiya Kamiyama[1] and Satoru Todo[1]

1 Department of General Surgery, Hokkaido University Graduate School of Medicine, Sapporo, Japan
2 Laboratory of Cancer Research, Department of Pathology, Hokkaido University Graduate School of Medicine, Sapporo, Japan
3 Department of Molecular Surgery, Hokkaido University Graduate School of Medicine, Sapporo, Japan
4 Faculty of Pharmaceutical Sciences, Hokkaido University, Sapporo, Japan

Summary

Since prolonged cold preservation of the heart deteriorates the outcome of heart transplantation, a more protective preservation solution is required. We therefore developed a new solution, named Dsol, and examined whether Dsol, in comparison to UW, could better inhibit myocardial injury resulting from prolonged cold preservation. Syngeneic heterotopic heart transplantation in Lewis rats was performed after cold preservation with UW or Dsol for 24 or 36 h. In addition to graft survival, myocardial injury, ATP content, and Ca^{2+}-dependent proteases activity were assessed in the 24-h preservation group. The cytosolic Ca^{2+} concentration of H9c2 cardiomyocytes after 24-h cold preservation was assessed. Dsol significantly improved 7-day graft survival after 36-h preservation. After 24-h preservation, Dsol was associated with significantly faster recovery of ATP content and less activation of calpain and caspase-3 after reperfusion. Dsol diminished graft injury significantly, as revealed by the lower levels of infarction, apoptosis, serum LDH and AST release, and graft fibrosis at 7-day. Dsol significantly inhibited Ca^{2+} overload during cold preservation. Dsol inhibited myocardial injury and improved graft survival by suppressing Ca^{2+} overload during the preservation and the activation of Ca^{2+}-dependent proteases. Dsol is therefore considered a better alternative to UW to ameliorate the outcome of heart transplantation.

Introduction

Graft dysfunction in the early phase of reperfusion, due to ischemia and reperfusion injury (IRI), is still the critical problem to be conquered in clinical heart transplantation [1]. Since the heart is susceptible to cold IRI [2], the time limit for a safe heart graft is 4–6 h in clinical settings using University of Wisconsin solution (UW) [3]. Improvement of the graft quality after cold preservation is thus a very important issue, but the method of cardiac cold preservation has not been dramatically changed since the UW was introduced in 1988 [4]. For this reason, a better, alternative organ preservation solution is needed.

During cold preservation, harmful processes such as ATP depletion [5], Ca^{2+} overload [6], production of reactive oxygen species (ROS) [7], cellular acidosis [8], swelling [9], and cytoskeletal disruption [10] are initiated and progress. During subsequent re-warming ischemia and reperfusion, some of these harmful cascades, including ROS production, Ca^{2+} overload and downstream

activation of proteases [11], and delayed recovery of ATP production [12], are further enhanced. Prolonged cold preservation exacerbates these processes, and eventually causes cardiac graft injury.

We therefore developed Dsol, a novel organ preservation solution based on UW solution with a high sodium and low potassium component, modified impermeants, and deuterium oxide (D_2O) as solvent (Table 1). We expect the extracellular-type composition of this solution without hydroxyethyl starch (HES) to inhibit coronary endothelial injury and subsequent graft infarction after reperfusion [13,14]. In addition, the impermeants sucrose and mannitol, which cost less than raffinose, are expected to give the solution potent cellular protection and antioxidant effects [15,16]. Deuterium oxide (D_2O) has unique biological effects, including inhibition of cytosolic Ca^{2+} overload [17], and the stabilization of microtubules [18], actin cytoskeleton [19], plasma membrane [20], and membrane-bound proteins [21]. D_2O also accelerates ATP production by stimulation of glucose uptake, glycolysis [22], and mitochondrial respiration [23]. These properties could suppress Ca^{2+}-induced cellular damage, and maintain structural and functional homeostasis of cardiomyocytes. In previous studies, the efficacy of D_2O for liver and heart preservation [24], and D_2O-containing solutions for kidney [25], pancreas [26], and vascular tissue preservation [27] has been reported. However, the effects of D_2O-containing solution have not yet been explored in a heart preservation and transplantation model.

The aims of the present study were to test whether Dsol, in comparison to the widely accepted UW, could better inhibit myocardial injury in extended cold preservation and subsequent syngeneic transplantation of rat hearts.

Materials and methods

Chemicals and reagents

All the chemicals and reagents were of the highest grade commercially available, and purchased from Wako Pure Chemical Co. (Osaka, Japan) unless otherwise noted.

Preparation of preservation solutions

UW solution (Viaspan®) was purchased from Bristol–Myers Squibb Co. (New York, NY, USA). Dsol was developed in our laboratory (Table 1). Deuterium oxide was purchased from Cambridge Isotope Laboratories (Andover, MA, USA). The freezing point of Dsol was 0.3 °C and we confirmed that Dsol would not freeze at 4 °C under the conditions employed herein. All solutions were filtered (0.45 μm) before use.

Animals

The experiments were approved by the institutional Animal Care Committee, and were conducted under the guidelines for animal care and use of Hokkaido University. Inbred male Lewis (LEW) rats weighing 250–350 g were purchased from Kyudo Co., Ltd. (Saga, Japan), and were used as both donors and recipients. They were maintained in a specific pathogen-free facility, and were used for the experiments without fasting.

Cell culture and reagents

H9c2 cells (passage 18–25; CRL-1446™; American Type Culture Collection, Rockville, MD, USA) were cultured in DMEM (Sigma–Aldrich, St. Louis, MO, USA) supplemented with 10% (v/v) heat inactivated bovine serum (Gibco–Invitrogen, Carlsbad, CA, USA), and penicillin–streptomycin (Gibco), under 95% air/5% CO_2 at 37 °C. To assess the cytosolic Ca^{2+} concentration, a FRET-based Ca^{2+} indicator, the Premo Cameleon Calcium Sensor™ (Molecular Probes Inc. Eugene, OR, USA), was transduced into the H9c2 cells according to the manufacturer's instructions. Briefly, the cells were incubated in a growth medium containing an appropriate amount of vector at room temperature for 4 h, then incubated for another 16 h in a fresh growth medium containing expression-enhancer solution. Cells (4×10^4 cells/well) were plated on a 96-well culture plate for fluorescent measurement overnight under the normal growth conditions.

Table 1. Composition of the preservation solutions.

	Dsol	UW
Additives (mM)		
NaOH	125	25
KOH	–	100
$MgSO_4$	5	5
KH_2PO_4	25	25
Lactobionate	100	100
Raffinose	–	30
Sucrose	20	–
Mannitol	10	–
Adenosine	5	5
Allopurinol	1	1
Glutathione	3	3
HES (g/l)	–	50
Solvent (%)		
H_2O	70	100
D_2O	30	–
Freezing point (°C)	0.3	−0.9

HES, Hydroxyethyl starch.

Heterotopic cardiac transplantation

Heterotopic heart transplantation was performed as previously described [28]. Briefly, after anesthetization with isoflurane inhalation, sodium heparin (1000 U/kg) was intravenously administered to the donor. Then, the heart was perfused in situ with 4 °C UW or Dsol from the aorta. The heart was rapidly excised and preserved in each solution at 4 °C. Recipients underwent a mid-line abdominal incision after anesthesia. The ascending aorta and pulmonary artery of the donors were anastomosed to the recipient's infra-renal abdominal aorta and inferior vena cava, respectively. The warm ischemic time was strictly adjusted to 25 min.

Experimental protocol in vivo

The grafts were transplanted after 24-h cold preservation in UW or Dsol solution (UW24 or Dsol24 group, respectively), 36-h preservation in UW or Dsol solution (UW36 or Dsol36 group, respectively), or no preservation (non-preserved control: NPC group). Graft survival was followed for 7 days. In the 24-h preservation groups, rats were sacrificed at 1 and 24 h after reperfusion (R1h and R24h, respectively). Grafts at the end of 24-h cold preservation (CP24h) in UW and Dsol solution, and normal heart controls (NHC) were also sampled. Graft infarction, apoptosis, serum biochemistry, inflammatory cells infiltration, high energy phosphates content, calpain and caspase 3 activities were assessed. At 7 days after reperfusion, rats were sacrificed to examine the level of graft fibrosis.

Graft survival

Graft survival was examined by palpation through the abdominal wall by two independent examiners in a blinded manner. Graft loss was defined as total stasis or the absence of any wall movement by direct inspection.

Infarction

Cardiac infarct size was assessed at R1h and R24h by triphenyltetrazolium chloride (TTC) staining as previously described [29]. Briefly, the excised hearts were incubated for 12 min in 1.5% TTC (w/v) in PBS at 37 °C, and fixed in 10% formalin-PBS thereafter. After taking microscopic images, the infarct area was calculated using computerized planimetry.

Apoptosis

Graft apoptosis was assessed at R24h by terminal dUTP nick end-labeling (TUNEL) staining as previously described [30]. Nuclei were counterstained with hematoxylin. TUNEL-positive cells were counted in five randomly selected HPFs (magnification ×400) adjacent to the necrotic area, the so-called area at risk, in a blinded manner. Mononuclear cells, cells without myofiber, or cells located at the interstitium were excluded as inflammatory cells. Results were expressed as the average number of TUNEL-positive cells per single HPF.

Infiltration of polymorphonuclear neutrophils (PMNs) and monocytes

The numbers of infiltrating inflammatory cells were assessed by counting the number of PMNs and monocytes at R24h. The grafts were fixed in 10% formalin-PBS, embedded in paraffin, and stained with hematoxylin-eosin (HE) for the PMNs count. Graft samples were also embedded and frozen in an OCT compound. Immunohistochemical (IHC) staining for monocytes/macrophages was performed with a mouse anti-rat CD68 antibody (AbD Serotec, Oxford, UK). Then the samples were incubated with a biotinylated goat anti-mouse IgG secondary antibody (DAKO, Cambridge, UK) and streptavidin-biotin-peroxidase (DAKO) in sequence. Detection of antibody binding was performed with 3,3'-diaminobenzidine (DAKO). Cells were counterstained with hematoxylin.

The numbers of PMNs and monocytes/macrophages were counted in 10 randomly selected HPFs for each section.

High energy phosphates

The levels of tissue adenine nucleotides (ATP, ADP, AMP) before preservation, at the end of 24-h cold preservation, and at R1h were measured as previously described [5]. Grafts were snap-frozen and homogenized in 20 µl/mg of ice cold 0.3 M perchloric acid with 0.01% (w/v) EDTA using a Polytron homogenizer (Kinematica Inc., Bohemia, NY, USA). After centrifugation (2200 g, 10 min, 4 °C), the supernatant was neutralized by 5 N KOH. An aliquot (20 µl) was analyzed by HPLC (Eicom, Kyoto, Japan). The dry-to-wet weight ratio of the tissue was separately measured by lyophilization. Myocardial adenine nucleotides were expressed as micromole per gram dry weight (µmol/g dw). Total adenine nucleotide (TAN) was calculated as the sum of ATP, ADP, and AMP.

Fibrosis

Grafts excised at R7d were fixed in 10% formalin-PBS, embedded in paraffin, and stained with Masson's trichrome. After microscopic images were taken with a BIO-REVO BZ9100 fluorescence microscope (KEYENCE, Osaka, Japan), they were processed using computerized